Available online at www.sciencedirect.com
SCIENCE DIRECT®
Journal of Pharmaceutical and Biomedical Analysis 36 (2004) 711–719
JOURNAL OF PHARMACEUTICAL AND BIOMEDICAL ANALYSIS
www.elsevier.com/locate/jpba

Plasmon-waveguide resonance spectroscopy applied to three potential drug targets: cyclooxygenase-2, hepatitis C virus RNA polymerase and integrin αVβ3

Savitha Devanathan[a], Mark C. Walker[b,*], Zdzislaw Salamon[a], Gordon Tollin[a]

[a] *Department of Biochemistry and Molecular Biophysics, University of Arizona, Tucson, AZ 85721, USA*
[b] *Pfizer Global Research and Development, 700 Chesterfield Parkway West, Chesterfield, MO 63017, USA*

Received 4 June 2004; received in revised form 13 August 2004; accepted 27 August 2004
Available online 8 October 2004

Abstract

Plasmon-waveguide resonance (PWR) spectroscopy has been used to study the interactions between ligands that correspond to inhibitors, activators or substrates and three integral membrane proteins representing potential drug targets; cyclooxygenases 1 and 2 (COX-1 and -2), integrin αVβ3, and hepatitis C virus RNA polymerase. The proteins were incorporated into an egg phosphatidylcholine bilayer deposited onto the surface of the PWR resonator, and changes in the amplitude and position of the PWR spectra due to mass density increases and conformational transitions have been used to characterize the kinetics and binding affinities corresponding to these interactions. Although the partition of COX-2 into the bilayer was not as efficient as was the case with the other two proteins, sufficient protein could be incorporated to allow ligand binding to be observed. It was also possible to incorporate COX-1 into a lipid bilayer by adding a suspension of microsomal membrane fragments containing this enzyme to a preformed bilayer, and to observe binding of an inhibitory ligand. The interactions between integrin αVβ3 and two ligands with different in vivo efficacies could be distinguished by both spectral measurements and binding kinetics. In the case of the RNA polymerase, the kinetics of PWR spectral changes upon adding a substrate solution to an enzyme–template complex were consistent with those obtained from direct measurements of enzymatic turnover. These experiments demonstrate the utility of PWR spectroscopy to provide novel information regarding drug interactions with membrane proteins in a lipid environment and to distinguish conformational changes induced by binding of various drug molecules.

Keywords: Plasmon-waveguide resonance spectroscopy; Label free spectroscopic technique; Conformational changes; Structural anisotropy; Binding kinetics

1. Introduction

Previous work from this laboratory [1–5] has utilized a recently developed spectroscopic method called plasmon-waveguide resonance (PWR) to investigate ligand and G-protein binding to members of the superfamily of 7-transmembrane helix GPCRs (δ-opioid and β_2-adrenergic receptors). PWR is able to determine binding constants and to characterize conformational states, with high sensitivity and without the need for radioactive or fluorescent labels. These experiments have provided new insights into the functional mechanisms of these integral membrane proteins, as well as demonstrating the potential usefulness of this technique in drug discovery. In the present studies, this methodology has been applied to members of three additional types of membrane-associated proteins, a monotopic enzyme having amphiphilic helices that attach it to one face of the lipid bilayer (cyclooxygenases 1 and 2, COX-1 and -2), an enzyme with a single C-terminal transmembrane helix anchoring it

Abbreviations: COX, cyclooxygenase; MBD, membrane binding domain; PGs, prostaglandins; Tx, thromboxanes; NSAIDs, non-steroidal anti-inflammatory drugs; DMSO, dimethyl sulfoxide; Tris, tris(hydroxymethyl) aminomethane; HCV, hepatitis C virus; PWR, plasmon-waveguide resonance

* Corresponding author. Tel.: +1 636 247 6572; fax: +1 636 247 7223.
E-mail address: mark.c.walker@pfizer.com (M.C. Walker).

0731-7085/$ – see front matter © 2004 Elsevier B.V. All rights reserved.
doi:10.1016/j.jpba.2004.08.030

to the membrane (hepatitis C virus RNA polymerase), and a receptor having two transmembrane helices (integrin αVβ3). This extends the range of potential drug targets for which useful new information can be obtained by PWR spectroscopy.

Prostaglandin H_2 synthases (PGHS), also known as cyclooxygenases (COX), catalyze the first committed step in the biosynthesis of prostaglandins (PG) and thromboxanes (Tx) via the bis-oxygenation of arachidonic acid. They are the pharmacological targets of non-steroidal anti-inflammatory drugs (NSAIDs) [6]. The inhibition of COX-2 derived PG production is thought to be responsible for the anti-pyretic, anti-inflammatory, and analgesic properties of NSAIDs and is, therefore, of great interest to the pharmaceutical industry.

Integrins are a class of heterodimeric cell surface receptors that mediate cell adhesion and migration, activation of intracellular kinase cascades, and gene transcription [7,8]. They have been implicated in the progression of a variety of diseases and hereditary disorders [9]. The dimeric unit is comprised of an α subunit of approximately 180 kD and a β subunit of approximately 90 kD. Each of these subunits are products of larger gene families which can associate to form distinct heterodimeric pairs. The α and β subunits are non-covalently linked integral membrane proteins that fold to form a large extracellular ligand binding domain [10,11]. Two transmembrane helices, contributed by each of the different subunits, serve to anchor the receptor to the membrane. A relatively small cytosolic domain serves to mediate bidirectional signaling, from the extracellular surface to the cytoplasmic interior (so called "outside-in") as well as from the cell interior to the extracellular environment ("inside-out" [12]). The latter of these reflects the activation state of the cell and serves to increase the integrin's affinity for extracellular ligands.

The hepatitis C virus (HCV) is an enveloped positive-stranded RNA virus belonging to the *Flaviviridae* family [13] that is replicated in the cytoplasm of the infected cell via minus-strand RNA intermediates. HCV is a major causative agent of sporadic and transfusion-associated liver disease. The genome composed of 9600 nucleotides encodes for at least 10 different cleavage products, three structural proteins and six non-structural proteins. One of the non-structural proteins (NS5B) of the HCV is an RNA-dependent RNA polymerase essential for replication of the viral genome [14,15] and is one of the main potential targets for anti-HCV agents. Enzymatic functions residing in the HCV non-structural proteins have become the focus of intensive research in search of efficient antiviral therapies. Recently published crystal structures of the HCV NS5B indicates that this enzyme adopts a unique overall structure with a fully encircled active site cavity rather than an open form like human immunovirus type 1 (HIV-1) or other polymerases [16–18]. Initiation of nucleotide polymerization is the most complex process of a polymerase cycle. Polymerases use a variety of strategies for initiation, including protein priming, oligonucleotide extension and de novo initiation. Detailed kinetic information is expected to play a crucial role in understanding the molecular basis of HCV NS5B-catalyzed nucleotide incorporation and subsequently the mechanistic characterization of the inhibitors.

In the work to be described further, PWR is able to detect spectral shifts accompanying ligand, substrate, or inhibitor binding to the purified membrane proteins studied here and, in the case of COX-1, to microsomal membrane fragments following incorporation of these materials into an egg phosphatidylcholine bilayer deposited onto the resonator surface. Binding occurs within concentration ranges consistent with the known affinities of the various interactions. Examples will be given of dose–response curves and of the kinetics of the events associated with the binding processes and with enzymatic turnover. The results demonstrate the utility of PWR in investigating these systems.

2. Materials and methods

2.1. Materials

Hematin and all standard buffer reagents were obtained from Sigma Chemical (St. Louis, MO). COX-1 from sheep seminal vesicles and recombinant murine COX-2 were purified as described previously [19]. The COX inhibitors, Celecoxib and SC-560, were prepared as described by Penning et al. [20] and supplied as solids. Their structures are shown in Fig. 1. Inhibitor stocks were prepared in DMSO. The human integrin, αVβ3, was obtained from

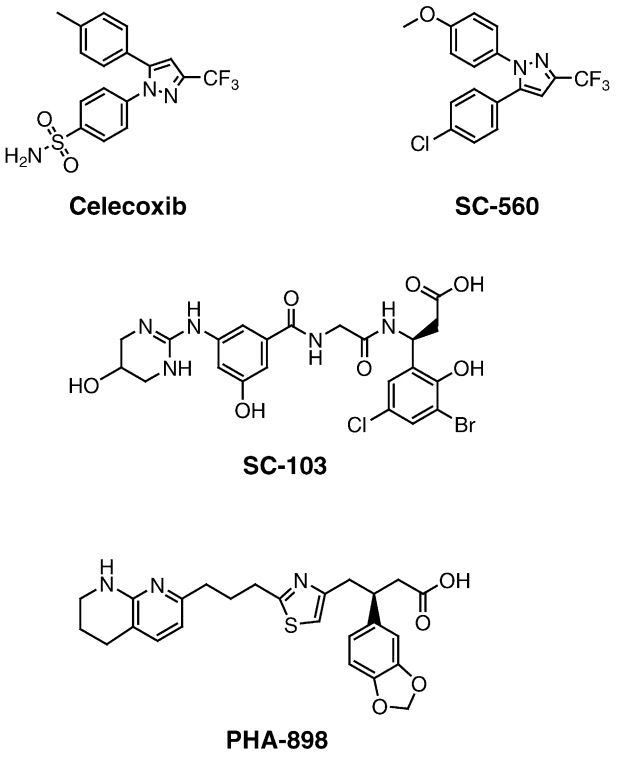

Fig. 1. Structures of ligands used in the present study.

Chemicon International Inc., (Temecula, CA) and was used without further purification. The hexapeptides, H_3N-Gly-Arg-Gly-Asp-Ser-Pro–COOH and H_3N-Gly-Arg-Ala-Asp-Ser-Pro–COOH, were obtained from EMD Biosciences Inc. (San Diego, CA). The small-molecule antagonists for the αVβ3 integrin, SC-103 and PHA-898, were provided by the Pfizer Medicinal Chemistry Department as the hydrochloride salts. Their structures are provided in Fig. 1.

Recombinant full length NS5B polymerase with a C-terminal 6-His tag was expressed using the baculovirus Sf9 cell system [15]. Purified protein was a kind gift from Pharmacia (Kalamazoo) and used without further purification. The polymerase was solubilized using 2% CHAPS detergent and purified using immobilized nickel affinity chromatography. Catalytic functionality of the full-length RNA polymerase was demonstrated using a homo-polymeric RNA template, as well as a hetero-polymeric RNA template, using the assay method described by Luo et al. [21]. The synthetic RNA hetero-polymer consisted of a random sequence of 32 nucleotides and was designed to be devoid of secondary structure. A mixture of GTP, ATP, CTP and UTP in buffer was used for de novo initiation with this template [22]. This hetero-polymeric 32-mer template was also utilized in the PWR experiments.

2.2. PWR spectroscopy

The physical basis of PWR spectroscopy has been described in detail elsewhere [3,23,24]. Briefly, PWR involves excitation of plasmon and waveguide modes by light from a polarized CW laser (He–Ne; λ = 543.5 or 632.8 nm) in a resonator consisting of a prism coated with silver and silica layers in contact with an aqueous compartment (Fig. 2). PWR spectra are measured by rotating the resonator with respect to the laser source and recording reflected light intensity as a function of incident angle. Resonance occurs at an angle slightly above the critical angle for total internal reflection, and is influenced by the refractive indices (n) and optical extinction coefficients (k) of the materials immobilized on the resonator surface, as well as by the thickness (t) of the deposited layer. Since resonances can be obtained with both *p*-polarized (electric vector perpendicular to the resonator surface) and *s*-polarized (electric vector parallel to the resonator surface) excitation, PWR spectra are sensitive to changes in both mass density and molecular orientation for materials deposited in ordered arrays on the resonator, as is the case with lipid bilayers containing incorporated integral proteins. Mass density changes result in isotropic alterations in PWR spectra, i.e. *p*- and *s*-polarized spectra shift by equal amounts in the same direction. Structural changes lead to anisotropic changes in PWR spectra, i.e. *p*- and *s*-polarized spectral shifts occur with unequal amplitudes, often in opposite directions. Graphical procedures have been developed to analyze these changes [25]. In the present systems, the materials do not absorb light at the excitation wavelengths used, and thus the k parameter has only a minor influence on the spectra (due mainly to light scattering by imperfections in the films).

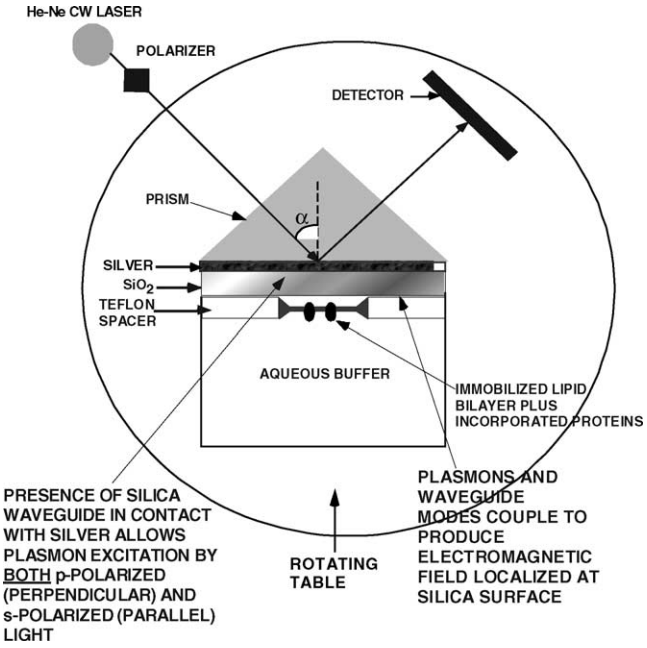

Fig. 2. Schematic diagram of the sample arrangement in a PWR apparatus. Polarized light (*p*- or *s*-polarization) from a CW laser is incident on the back surface of a silver film at an angle (α) slightly above the critical angle for total internal reflection. This causes plasmon and waveguide modes to be excited, resulting in an evanescent electromagnetic field localized at the outer surface of the silica layer. Molecules immobilized at the interface between this surface and the aqueous compartment interact with this field, thereby altering the resonance excitation process. This is detected by changes in the intensity of the light reflected by the silver layer, measured as a function of the incident angle (PWR spectrum).

In the experiments described herein, plasmon resonance spectra were obtained using a Beta PWR instrument obtained from Proterion Corp. (Piscataway, NJ) that records the relative reflectance versus the absolute angle with a resolution of 1 mdeg. Immobilized protein samples were prepared by adding microliter aliquots of either detergent-solubilized proteins or membrane fragments to the aqueous compartment of the PWR cell containing an appropriate buffer of approximately 1 ml total volume. This addition resulted in dilution of the detergent to below the critical micelle concentration and spontaneous incorporation of the protein into an egg phosphatidylcholine bilayer already deposited onto the resonator surface and in contact with the aqueous buffer (Salamon et al., for details of bilayer formation) [3,26]. Protein incorporation into the bilayer was monitored by changes in the PWR spectra that were followed in real time until equilibrium was established (usually 10–20 min). In most cases several aliquots were added, although complete saturation was generally not achieved. Subsequent to protein incorporation, microliter aliquots of ligand or substrate solutions were added and the resulting changes in the PWR spectra were again monitored as a function of time. In some experiments, saturating amounts were added so as to follow the kinetics of

Table 1
PWR resonance shifts occurring upon successive additions of various integral membrane proteins and ligands to an egg PC bilayer

Protein	Conditions	*p*-Shifts (mdeg)	*s*-Shifts (mdeg)
COX-2	+Apoprotein	11	8
	+Hemin	12	8
	+Ligand (celecoxib)	36	25
COX-1	+Membrane fragments	9	8
	+Ligand (SC-560)	11	11
Integrin – αVβ3			
Peptide experiment			
	+Integrin	31	36
	+RGD hexapeptide	7	8
PHA-898 plus SC-103			
	+Integrin	42	53
	+PHA-898	18	12
	+SC-103	11	9
SC-103 plus PHA-898			
	+Integrin	13	17
	+SC-103	8	10
	+PHA-898	7	7
HCV RNA polymerase			
	+Polymerase	27	24
	+32-nt template	12	9
	+NTP	−16	−17

The errors in these values are ±1 mdeg.

ligand binding whereas, in other experiments, several aliquots of sub-saturating amounts were successively added in order to obtain a dose–response curve. The PWR spectral shifts observed in these experiments are summarized in Table 1. The standard deviations of these shifts are ±1 mdeg, as determined from replicate measurements.

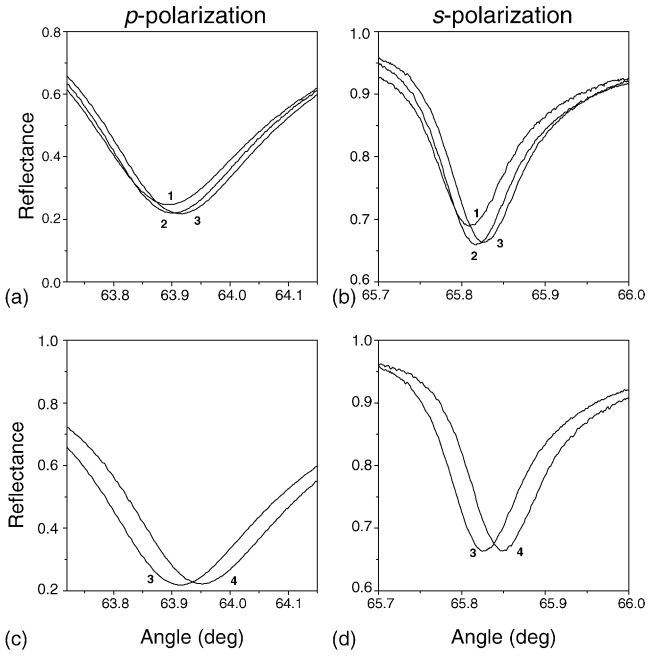

Fig. 3. *Top*: PWR spectra of an egg PC bilayer in contact with a 10 mM Tris, 10 mM KCl, pH 7.3 buffer (curves 1) for *p*- (left panel) and *s*-polarization (right panel). Addition of COX-2 apoprotein dissolved in buffer containing 30 mM octylglucoside to the aqueous cell compartment (final protein concentration = 12.6 (M) shifted both the *s*- and *p*-polarized spectra to larger incident angles with an increase in spectral depth (curves 2). Addition of a hemin solution (final concentration = 10 μM) in DMSO to the incorporated apoprotein resulted in additional spectral shifts to higher incident angles (curves 3). *Bottom*: Addition of an ethanol solution of the COX-2 selective ligand celecoxib (final concentration = 1 μM) to the PWR cell containing incorporated holoprotein (curves 3 are the same as those in the top panel) resulted in shifts to larger incident angles for both *s*- and *p*-polarized spectra (curves 4), with no significant changes in the spectral depth.

3. Results

3.1. Binding of inhibitors to COX-1 and -2

Fig. 3 shows the results obtained following the addition of COX-2 apoprotein, solubilized in an octylglucoside-containing buffer, to the aqueous compartment of a PWR cell within which a lipid bilayer had previously been deposited onto the resonator surface. Protein insertion into the bilayer was clearly evident from the changes in the intensity and angular positions of the *s*- and *p*-polarized resonances. Control experiments (not shown) demonstrated that the addition of octylglucoside-containing buffer alone did not cause any spectral changes. Note that the amounts of COX-2 that were required in order to obtain these effects were relatively large and the PWR spectral shifts were rather small, as compared to results with other membrane proteins both in the present experiments (see further) and in previous investigations [4,5,23,26,27]. This comparison suggests that the efficiency of COX-2 incorporation into the bilayer was low, which perhaps is not surprising considering that the COX protein is a monotopic integral membrane protein with only a relatively small hydrophobic membrane-binding domain. In contrast to the small changes observed in the incident angle position, the relatively large changes in spectral intensity are suggestive of an appreciable structural anisotropy induced in the bilayer by COX-2 insertion. This is also not surprising, given that most of the protein extends outside of the membrane in this system [28–30].

Following incorporation of the COX apoprotein into the bilayer, a microliter aliquot of a dimethylsulfoxide solution of hemin was added to the aqueous compartment to produce the holoprotein. An additional spectral shift was observed (Fig. 3a and b) that probably reflects both mass density and conformational alterations upon formation of the holoprotein. The addition of the COX-2 selective inhibitor, celecoxib, at concentrations expected to saturate the active site (IC_{50} ∼0.03 μM [31]) produced further PWR spectral changes (Fig. 3c and d), again due to both mass density and conformational changes accompanying ligand binding. Control experiments (not shown) demonstrated that these spectral changes were only produced when COX-2 was present in the membrane. Similar results upon celecoxib binding were

obtained in experiments in which hemin was added to the apoprotein prior to insertion into the bilayer.

COX-2 is quite soluble in aqueous buffer even at low concentrations of octylglucoside, as evidenced from the relatively low efficiency of incorporation into the bilayer. In a separate experiment, excess COX-2 was removed by flushing the sample compartment with fresh buffer following protein incorporation. The results obtained demonstrated that the ligand-induced spectral shifts were not due to insertion of protein into the membrane upon binding of celecoxib to COX in the bulk solvent (data not shown).

The incorporation of membrane proteins as part of a crude microsomal fraction was demonstrated using COX-1 that was over expressed in insect cells. As is evident in Fig. 4, the membrane fragments either fused with, or adsorbed onto, the egg PC bilayer that had been previously deposited on the resonator surface. Furthermore, sufficient COX-1 was present on the PWR resonator to produce spectral shifts (Fig. 4) upon addition of a saturating amount of a COX-1 specific inhibitor, SC-560 (IC_{50} ~0.0005 μM [31]). This result clearly demonstrates that PWR experiments can be performed using membrane preparations obtained from cells over expressing recombinant proteins, without the necessity of extensive isolation and purification.

3.2. Ligand binding to integrin αVβ3

PWR spectral changes produced upon addition of an octylglucoside-containing solution of integrin to the aqueous compartment of a cell containing a previously deposited egg PC bilayer are shown in Fig. 5. Note that considerably smaller protein concentrations were used and larger spectral shifts were produced, indicating higher incorporation efficiency than was observed with COX-2. This result is consistent with the transmembrane nature [32,33] of the integrin molecule, and demonstrates an appreciably higher affinity for the bilayer. Incorporation of the integrin into the bilayer

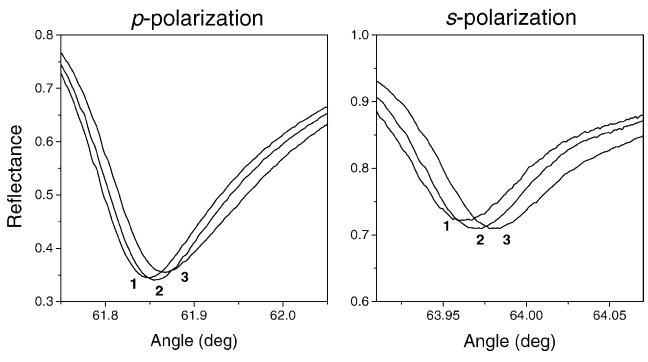

Fig. 4. PWR spectrum of an egg PC bilayer in contact with a 10 mM Tris, pH 7.3, buffer before (curves 1) and after (curves 2) a microsomal membrane fraction containing COX-1 was added to the aqueous compartment. Shifts to larger incident angles were observed. Addition of an ethanol solution of SC-560 (a COX-1 selective ligand) to the PWR aqueous compartment (final concentration = 1.5 (M) resulted in further spectral shifts to larger angles (curves 3) with small anisotropic changes in spectral depth.

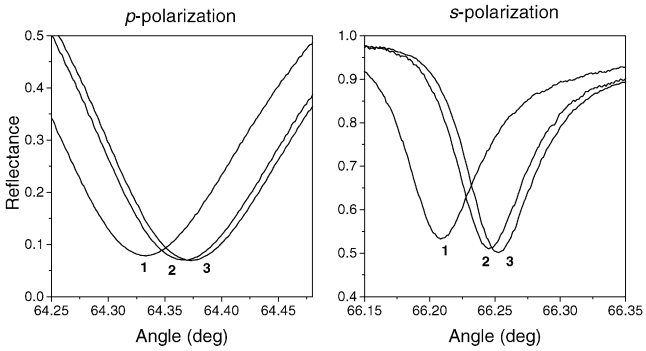

Fig. 5. PWR spectra obtained after depositing onto the resonator surface an egg PC bilayer in contact with a buffer containing 10 mM Tris, pH 7.3, and 1 mM $MgCl_2$ (curves 1), and after adding human integrin αVβ3 in 10 mM octyl glucoside (final protein concentration = 54 nM) (curves 2). Incorporation of protein produced shifts to larger incident angles and changes in spectral depth for both *s*- and *p*-polarized spectra. After incorporation, an aliquot of RGD peptide was added into the sample cell (final concentration = 2 nM) resulting in further increases in the spectral incident angles and spectral depths (curves 3).

results in anisotropic spectral changes, with *s*-shifts larger than *p*-shifts (see Table 1 for values), indicating the occurrence of structural changes in the proteolipid membrane. The addition of a solution of hexapeptide containing the αVβ3 recognition sequence, RGD, to the sample cell produced an additional spectral shift. Addition of aliquots of this peptide caused progressive shifts that define a hyperbolic curve, yielding a binding constant of 0.10 nM (Fig. 6). This example illustrates the high sensitivity of the PWR methodology. High affinity binding of the RGD peptide to human αVβ3 integrin has been observed previously (K_D = 14 nM; data not shown) in separate experiments using a solid phase assay involving αVβ3-coated plates [34]. The greater affinity demonstrated for the RGD peptide in the present study may

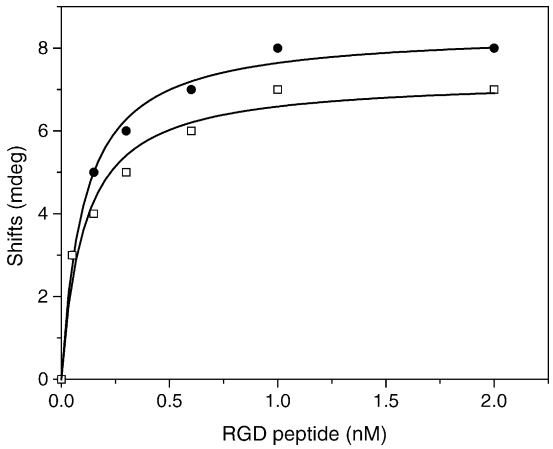

Fig. 6. Titration curve showing PWR spectral shifts occurring upon addition of aliquots of RGD peptide (concentration range was 50 pM–2 nM) to bilayer-incorporated integrin αVβ3. Solid curves are hyperbolic fits to the *p*- (□) and *s*-polarized (●) spectral data with K_D values of 0.10 ± 0.01 nM. Conditions were as in Fig. 5.

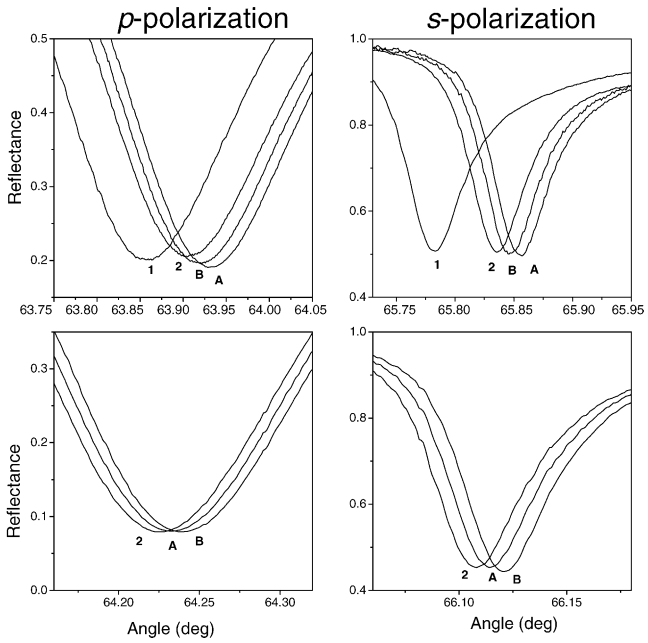

Fig. 7. *Top*: PWR spectra for an egg PC bilayer in 10 mM Tris, pH 7.3, and 1 mM $MgCl_2$ before (curves 1), and after integrin αVβ3 (final concentration = 58.5 nM) in 10 mM octylglucoside was added (curves 2) causing shifts to larger incident angles. PHA-898 (final concentration = 500 nM) was then added to the sample cell (curves B), resulting in a further increase in resonance angle position for both *p*- and *s*-polarized spectra and a slight increase in depth for the *p*-polarized spectrum. Subsequent addition of SC-103 (final concentration = 10 (M) resulted in additional spectral shifts to larger angles for both *s*- and *p*-polarized spectra and a further small increase in spectral depth for *p*-polarization (curves A). *Bottom*: PWR spectra for integrin αVβ3 after incorporation into an egg PC bilayer (curves 2), and after addition of SC-103 (final concentration = 10 (M) (curves A), followed by addition of PHA-898 (final concentration = 500 nM) (curves B). Conditions were as in top panel.

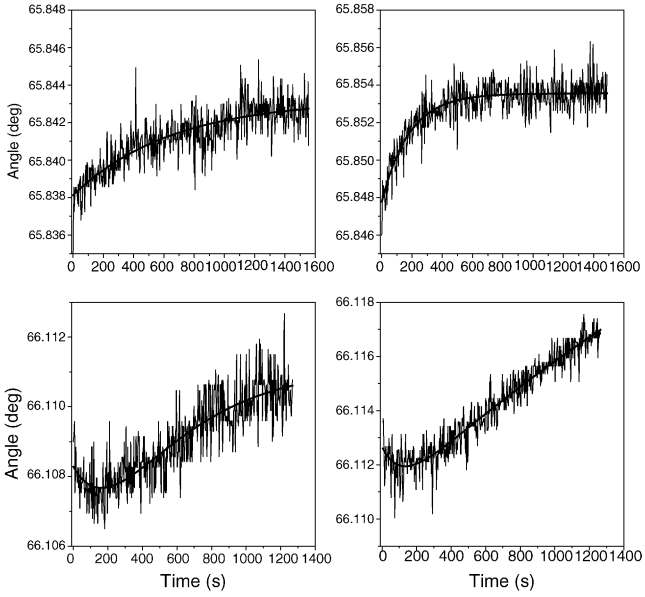

Fig. 8. *Top left*: Kinetics of binding of PHA-898 (final concentration = 500 nM) to bilayer-incorporated integrin αVβ3 plotted as spectral position vs. time. Conditions were as in Fig. 7. Solid line is a single exponential fit to the kinetic data yielding a rate constant of $1.1 \times 10^{-3}\,s^{-1}$. *Top right*: Kinetics of the subsequent binding of SC-103 (final concentration = 10 (M) to PHA-898-ligated integrin plotted as spectral position vs. time. Conditions were as in Fig. 7. Solid line is a single exponential fit to the data with a rate constant of $3.8 \times 10^{-3}\,s^{-1}$. *Bottom left*: Kinetics of binding of SC-103 (final concentration = 500 nM) to bilayer-incorporated integrin αVβ3 plotted as spectral position vs. time. Data were fit with two exponentials (solid line) with rate constants of $2.4 \times 10^{-3}\,s^{-1}$ and $1.9 \times 10^{-3}\,s^{-1}$. *Bottom right*: Kinetics of the subsequent binding of PHA-898 (final concentration = 10 (M) to SC-103-ligated integrin plotted as spectral position vs. time. Data were fit with two exponentials (solid line) with rate constants of $6.1 \times 10^{-3}\,s^{-1}$ and $0.22 \times 10^{-3}\,s^{-1}$.

reflect the ability of integrin to adopt a more physiologically relevant conformation when reconstituted in a lipid bilayer. The K_D value obtained here is also in satisfactory agreement with results obtained for the binding of the RGD-containing peptide, echistatin, to purified αVβ3 in an in vitro assay (K_D = 0.5 nM [35]).

Figs. 7 and 8 demonstrate the ability of PWR to distinguish between two synthetic integrin-specific ligands having different in vivo efficacies by experiments in which the two ligands were added successively to an integrin-containing bilayer. When a saturating amount of PHA-898 (IC_{50} = 1.4 nM [34]) was added to a PWR cell containing bilayer-incorporated integrin, a shift to larger incident angles, and an increase in spectral depth for the *p*-polarized resonance, was observed (Fig. 7, top). A similar result was obtained in a separate experiment upon addition of an excess of SC-103 (IC_{50} = 0.85 nM [34]) to an integrin sample (Fig. 7, bottom), although in this case no significant change in spectral depth was observed for either resonance. Since the molecular weights of these two compounds are closely similar (PHA-898, MW = 502; SC-103, MW = 621), the differences in spectral response indicate that different conformations of the integrin were produced upon binding of these two ligands. Subsequent additions of saturating amounts of PHA-898 or SC-103 in these two experiments produced further shifts to larger angles (Fig. 7, top and bottom). This indicates that PHA-898 and SC-103, respectively, were displaced from the integrin by the second addition. Again, since mass changes are not likely to be responsible for the additional spectral shifts, this further suggests that the two ligands generated different conformations of the protein. This is also shown by the fact that the changes in spectral depths upon binding these two ligands to integrin were different (compare top and bottom panels for both polarizations). The spectral shift values (Table 2) are also consistent with this. Thus, upon addition of the ligand PHA-898, spectral changes occur in which *p*-shifts are larger than *s*-shifts and the *p*-spectrum becomes deeper than the *s*-spectrum. Subsequent addition of the ligand SC-103 shows a further *p*-shift that is larger than the *s*-shift. However, reversing the order of addition of SC-103 results in *s*-shifts larger than *p*-shifts, which is different from that obtained upon addition of PHA-898. These changes clearly demonstrate that different conformational states are produced by these two ligands.

The kinetics of the binding processes for the two ligands are presented in Fig. 8. The shifts to larger angles obtained upon PHA-898 addition to the incorporated integrin, followed by SC-103 addition, could both be fit with a single exponential function, although the rate constants were not the same. However, both the kinetic curves for SC-103 addition and the subsequent addition of PHA-898 were biphasic, with a small negative shift followed by a larger positive shift, again with apparently different rate constants. This demonstrates that these two ligands produce different conformations upon binding, and that the binding mechanisms were also different.

3.3. Binding of RNA template to hepatitis C virus RNA polymerase and enzymatic synthesis of oligonucleotide

Appreciable shifts of the *p*- and *s*-polarized PWR spectra to larger incident angles occurred when a solution of HCV (recombinant hepatitis C virus) RNA polymerase in buffer containing 2% CHAPS was added to the aqueous compartment of the PWR instrument in which an egg PC bilayer had previously been deposited on the resonator surface (Fig. 9).

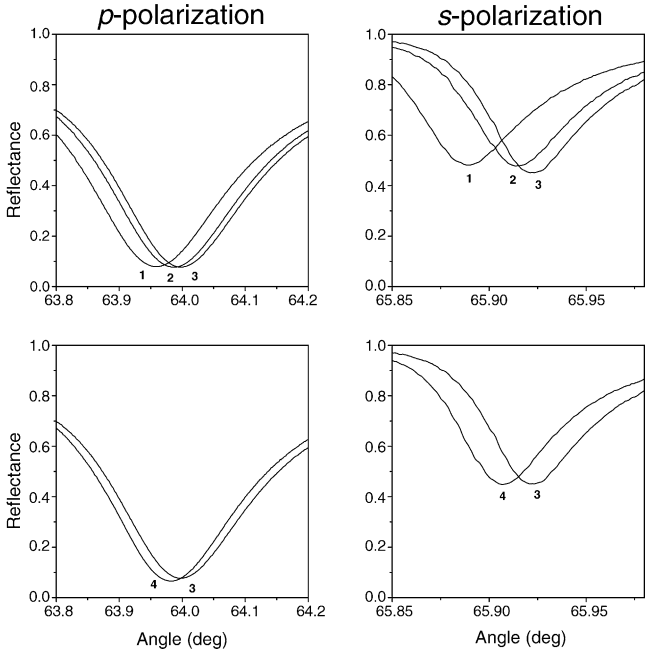

Fig. 9. *Top*: PWR spectrum obtained with an egg PC bilayer deposited on the PWR resonator in contact with buffer containing 20 mM Tris, 100 mM ammonium acetate and 1 mM $MnCl_2$ (curves 1). Addition of a solution of HCV (hepatitis C virus-recombinant) RNA polymerase in buffer containing 2% CHAPS (final protein concentration = 50 nM) (curves 2) caused shifts to larger incident angles. A 32-mer RNA template was then added to the membrane-bound polymerase to a final concentration of 24 nM (curves 3), resulting in additional shifts to larger angles and an increase in depth for the *s*-polarized resonance. *Bottom*: An NTP mixture (GTP-50 μM; ATP, CTP, UTP-2 (M) was added to the sample cell (final concentration of the mixture = 1 (M) after the addition of the RNA template (curves 3 are the same as those in the top panel), which resulted in resonance shifts to lower incident angles (curves 4).

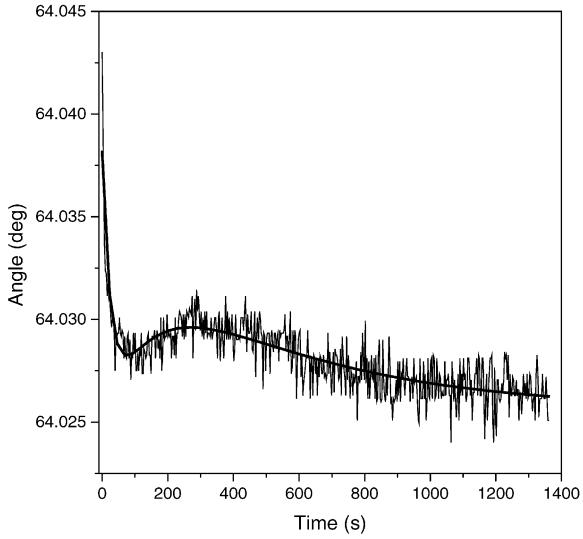

Fig. 10. The time course of NTP interaction with the template-bound RNA polymerase is shown as a plot of incident angle vs. time obtained for *s*-polarization. The kinetic pattern indicates at least three phases associated with enzymatic turnover to produce double-stranded RNA. The solid curve is a three-exponential fit to the data.

As was the case with integrin, only nanomolar concentrations of the polymerase were required in order to obtain significant incorporation, again consistent with the transmembrane nature of the protein. Addition of a solution of an RNA template to the aqueous phase of the PWR cell caused an additional spectral shift to larger angles (Fig. 9), consistent with an increase in mass caused by binding of the template to the polymerase. Subsequent addition of a solution containing a mixture of nucleoside triphosphates (predominantly GTP) to the cell caused a shift of the PWR spectra to smaller incident angles (Fig. 9). Such a negative shift can only be caused by structural changes, inasmuch as mass increases always result in refractive index increases which necessarily are reflected in positive angular resonance shifts.

Fig. 10 shows the time course of the negative shifts induced by NTP addition. Complex multiphasic kinetics were obtained as a result of NTP incorporation into the membrane bound RNA-polymerase complex. An initial fast binding step was observed resulting in a shift to lower incident angles. This was followed by a slower shift to larger angles and a still slower shift to shorter angles as the system came to a final equilibrium. A three-exponential fit to the experimental data yielded rate constants having values of 2.57 ± 0.26, 0.24 ± 0.03, 0.094 ± 0.006 min^{-1} (half-lives: t_1= 0.27 ± 0.03, t_2= 2.9 ± 0.4, t_3 = 7.4 ± 0.5 min), respectively (χ^2 = 9.1886E − 7). It is important to point out that the absolute values of the resonance angles shown in Figs. 9 and 10 are different. This is typical of PWR experiments done at different times with different bilayers and different resonators. The relative magnitudes of the shifts, rather than the absolute angles at which the resonances occur, is what is important

4. Discussion

The present investigation demonstrates the utility of PWR spectroscopy to examine ligand binding to membrane proteins of therapeutic interest that have been reconstituted in a lipid bilayer. Unlike other direct binding methods that utilize proteins that have been detergent solubilized, PWR can be used to explore the contribution of a lipid environment to drug binding and potency. Furthermore, the membrane proteins utilized have minimal interactions with the lipid bilayer, in contrast to those in previous studies [2–5]. These results expand the repertoire of membrane proteins amenable to investigation using PWR spectroscopy.

Results from X-ray crystallography [28,29] have demonstrated that the dimeric COX enzyme is comprised of an EGF-like domain, a membrane-binding domain (MBD), and a globular catalytic domain. The membrane-binding domain is comprised of four amphipathic helices that appear to associate with only one leaflet of the lipid bilayer. Results from photo-affinity labeling and mutagenesis studies [30] support this hypothesis. The helices of the membrane-binding domain form the mouth of a hydrophobic channel that extends 20 Å within the globular catalytic domain to the cyclooxygenase active site. Consequently, access to the cyclooxygenase active site by lipid substrates and inhibitors is likely mediated by interactions with the MBD and the lipid bilayer [28,29]. In the case of the detergent-solubilized enzyme, it seems likely that the mouth of the channel is more solvent exposed than for the membrane-associated enzyme and, therefore, more accessible to inhibitors present in solution. The ability to directly monitor ligand binding to COX reconstituted into a lipid bilayer could therefore provide new insight into the dependence of inhibitor potency on hydrophobicity, and a potential role of drug interactions with the membrane bilayer.

Integrins mediate bidirectional signaling across the plasma membrane. Recent structural studies have provided evidence for distinct conformational changes in the intracellular, transmembrane and extracellular domains [36], and have given additional insight into the complexity associated with signal transduction mediated by these structural changes. Activation and ligand binding events include interactions with cytoskeletal components and extracellular matrix proteins, as well as reorganization and clustering of the integrin subunits across the membrane surface [37]. The conformational changes, as well as larger structural reorganizations within the bilayer, provide a variety of opportunities for the development of small molecule antagonists. The results presented demonstrate that two integrin-specific ligands with different efficacy in vivo induce distinct conformational changes upon binding to the integrin. Furthermore, ligand binding and the resulting conformational changes were demonstrated to occur in a multi-step process, involving at least two kinetically distinct steps. Thus, the application of PWR to monitor changes in integrin conformation and structure within a lipid bilayer upon the binding of small molecule antagonists represents a unique approach for the development of new integrin-targeted therapeutics, which may thus prove useful in drug design protocols.

Efficient assembly of polymerase–RNA template complex is an essential step to permit nucleotide incorporation for determination of the kinetics of HCV NS5B-catalyzed RNA synthesis. In the experiments described above, a small synthetic RNA sequence (a 32 nucleotide RNA without any secondary structures such as a stem loop at the 3′-end) was used as a template to test for the ability of HCV NS5B to initiate RNA synthesis de novo by either folding back of the template intramolecularly upon binding to the polymerase for copy-back RNA synthesis or by synthesis of a complementary RNA strand [21]. The polymerase activity was observed here as changes in the PWR resonance position following GTP initiation. Subsequent to RNA binding, addition of GTP caused positive-strand synthesis resulting in PWR spectral shifts that demonstrate three distinct kinetic phases. This is in contrast to previous kinetic analysis, which has identified only two distinct phases that have been interpreted as initiation and chain elongation. The rapid change in resonance position to lower angles likely reflects enzyme structural changes occurring upon NTP binding. The subsequent slower changes could represent base pairing with the 3′-terminal template base of the viral RNA and the initiation of synthesis, followed by elongation of the complementary RNA strand to produce short transcripts. It has been shown in previous studies [21,38] that the base pairing step is sensitive to NTP concentration and is therefore rate-limiting. Furthermore, RNA synthesis using GTP has been shown by steady-state experiments to proceed via complex biphasic kinetics with k_{cat} values of $0.017 \pm 0.002\,min^{-1}$ and $0.086 \pm 0.003\,min^{-1}$. The latter value compares well with the slowest rate constant observed in the present PWR investigation ($0.094 \pm 0.006\,min^{-1}$) and thus supports the hypothesis that the changes observed likely correspond to RNA synthesis in these experiments. The fact that PWR allows a deconvolution of intermediate steps in enzyme turnover should allow its use in studies of drug interventions at various points along the reaction pathway.

The present studies demonstrate the utility of PWR spectroscopy to provide novel structural information regarding drug interactions with membrane proteins in a lipid environment. In the first example, COX represents an integral membrane protein in which the drug binding site is only accessible via the protein–lipid interface. PWR spectroscopy allows one to monitor ligand binding within the context of a lipid bilayer, which can provide insight regarding the contribution of the hydrophobic lipid phase to drug potency. In the second example, integrins mediate bi-directional signaling via conformational changes induced upon ligand binding at either the cytosolic or the extracellular side of the cell membrane. PWR can distinguish unique conformational changes induced upon ligand binding and thereby may provide insight into the pharmacological action of drug leads based upon the spectral changes observed. Finally, HCV polymerase provides an example of a membrane-associated enzyme that catalyzes a complex reaction sequence consisting of tem-

plate binding, initiation, and chain elongation steps during enzymatic turnover. PWR has permitted the identification of conformational changes associated with each stage of the catalytic cycle that could be exploited to develop novel targets for drug development. In each of these examples, the utility of PWR spectroscopy distinguishes this technique from currently available methods to provide important insights into protein–ligand interactions for drug discovery efforts.

Acknowledgments

The authors would like to acknowledge James Gierse for providing samples of purified recombinant COX-2 and microsomal fractions of ovine COX-1, and Roger Poorman for providing HCV RNA polymerase, RNA template and the NTP mixture. The authors would also like to thank Drs. David Griggs and G. Alan Nickols for helpful discussions concerning the αVβ3 integrin, and Dr. Peter Wells for helpful discussions and review of the manuscript with regards to HCV RNA polymerase.This work was supported by a National Institutes of Health grant R01-GM059630 (to G.T. and Z.S.).

References

[1] Z. Salamon, H.A. Macleod, G. Tollin, Biophys. J. 73 (1997) 2791–2797.
[2] Z. Salamon, S. Cowell, E. Varga, H.I. Yamamura, V.J. Hruby, G. Tollin, Biophys. J. 79 (2000) 2463–2474.
[3] Z. Salamon, V.J. Hruby, G. Tollin, S.M. Cowell, J. Peptide Res. 60 (2002) 322–328.
[4] I.D. Alves, Z. Salamon, E. Varga, H.I. Yamamura, G. Tollin, V.J. Hruby, J. Biol. Chem. 278 (2003) 48890–48897.
[5] S. Devanathan, Z. Yao, Z. Salamon, B. Kobilka, G. Tollin, Biochemistry 23 (2004) 3280–3288.
[6] L.J. Marnett, S.W. Rowlinson, D.C. Goodwin, A.S. Kalgutkar, C.A. Lanzo, J. Biol. Chem. 274 (1999) 22903–22906.
[7] F.G. Giancotti, E. Ruoslahti, Science (1999) 285.
[8] M.J. Humphries, Arthritis Res. 4 (2002) S69–S78.
[9] C.W. Hamm, Ann. Rev. Med. 54 (2003) 425–435.
[10] J.-P. Xiong, T. Stehle, B. Diefenbach, R. Zhang, R. Dunker, D.L. Scott, A. Joachimiak, S.L. Goodman, M.A. Arnaout, Science 294 (2001) 339–345.
[11] J.-P. Xiong, T. Stehle, R. Zhang, A. Joachimiak, M. Frech, S.L. Goodman, M.A. Arnaout, Science 296 (2002) 151–155.
[12] E.F. Plow, T.A. Haas, L. Zhang, J. Loftus, J.W. Smith, J. Biol. Chem. 275 (2000) 21785–21788.
[13] R.H. Miller, R.H. Purcell, Proc. Natl. Acad. Sci. USA (1990) 87.
[14] S.-E. Behrens, L. Tomei, R. De Francesco, EMBO J. 15 (1996) 12–22.
[15] V. Lohmann, F. Korner, U. Herian, R. Bartenschlager, J. Virol. 71 (1997) 8416–8428.
[16] H. Ago, T. Adachi, A. Yoshida, M. Yamamoto, N. Habuka, K. Yatsunami, M. Miyano, Structure 7 (1999) 1417–1426.
[17] S. Bressanelli, L. Tomei, A. Roussel, I. Incitti, R.L. Vitale, M. Mathieu, R. De Francesco, F.A. Rey, Proc. Natl. Acad. Sci. USA 96 (1999) 13034–13039.
[18] C.A. Lesburg, M.B. Cable, E. Ferrari, Z. Hong, A.F. Mannarino, P.C. Weber, Nat. Struc. Biol. 6 (1999) 937–943.
[19] J.K. Gierse, C.M. Koboldt, M.C. Walker, K. Seibert, P.C. Isakson, Biochem. J. 339 (1999) 607–614.
[20] T.D. Penning, J.J. Talley, S.R. Bertenshaw, J.S. Carter, P.W. Collins, S. Doctor, M.J. Graneto, L.F. Lee, J.W. Malecha, J.M. Miyashiro, R.S. Rogers, D.J. Rogier, S.S. Yu, G.D. Anderson, E.G. Burton, J.N. Cogburn, S.A. Gregory, C.M. Koboldt, W.E. Perkins, K. Seibert, A.W. Veenhuizen, Y.Y. Zhang, P.C. Isakson, J. Med. Chem. 40 (1997) 1347–1365.
[21] G. Luo, R.K. Hamatake, D.M. Mathis, J. Racela, K.L. Rigat, J. Lemm, R.J. Colonno, J. Virol. 74 (2000) 851–863.
[22] W. Zhong, A.S. Uss, E. Ferrari, J.Y.N. Lau, Z. Hong, J. Virol. (2000) 74.
[23] Z. Salamon, M.F. Brown, G. Tollin, Trends Biochem. Sci. 24 (1999) 213–219.
[24] Z. Salamon, G. Tollin, Surface plasmon resonance: theoretical principles, in: Encyclopedia of Spectroscopy and Spectrometry, Academic Press, New York, 1999.
[25] Z. Salamon, G. Tollin, Biophys. J. 86 (2004) 2508–2516.
[26] Z. Salamon, D. Huang, W.A. Cramer, G. Tollin, Biophys. J. 75 (1998) 1874–1885.
[27] Z. Salamon, G. Lindblom, L. Rilfors, K. Linde, G. Tollin, Biophys. J. 78 (2000) 1400–1412.
[28] D. Picot, P.J. Loll, R.M. Garavito, Nature 367 (1994) 243–249.
[29] R.G. Kurumbail, A.M. Stevens, J.K. Gierse, J.J. McDonald, R.A. Stegeman, J.Y. Pak, D. Gildehaus, J.M. Miyashiro, T.D. Penning, K. Seibert, P.C. Isakson, W.C. Stallings, Nature 384 (1996) 644–648.
[30] A.G. Spencer, E. Thuresson, J.C. Otto, I. Song, T. Smith, D.L. DeWitt, R.M. Garavito, W.L. Smith, J. Biol. Chem. 274 (1999) 32936–32942.
[31] J. Gierse, R. Kurumbail, M. Walker, B. Hood, J. Monahan, J. Pawlitz, R. Stegeman, A. Stevens, J. Kiefer, C. Koboldt, K. Moreland, S. Rowlinson, L. Marnett, J. Pierce, J. Carter, J. Talley, P. Isakson, K. Seibert, Mechanism of inhibition of novel COX-2 inhibitors, in: Proceedings of the Eicosanoids and Other Bioactive Lipids in Cancer, Inflammation, and Radiation Injury, vol. 2, Plenum Press, New York, 2002, pp. 365–369.
[32] R. Li, C.R. Babu, J.D. Lear, A.J. Wand, J.S. Bennett, W.F. DeGrado, Proc. Natl. Acad. Sci. USA 98 (2001) 12462–12467.
[33] O. Vinogradova, A. Velyvis, A. Velyviene, B. Hu, T. Haas, E. Plow, J. Qin, Cell 110 (2002) 587–597.
[34] V.W. Engleman, G.A. Nickols, F.P. Ross, M.A. Horton, D.W. Griggs, S.L. Settle, P.G. Ruminski, S.L. Teitelbaum, J. Clin. Invest. 99 (1997) 2284–2292.
[35] M. Yamamoto, J.E. Fisher, M. Gentile, J.G. Seedor, C.T. Leu, S.B. Rodan, G.A. Rodan, Endocrinology 139 (1998) 1411–1419.
[36] J. Takagi, T.A. Springer, Immunol. Rev. 186 (2002) 141–163.
[37] R. Li, N. Mitra, H. Gratkowski, G. Vilaire, R. Litvinov, C. Nagasami, J.W. Weisel, J.D. Lear, W.F. DeGrado, J.S. Bennett, Science 300 (2003) 795–798.
[38] W. Zhong, E. Ferrari, C.A. Lesburg, D. Maag, S.B. Ghosh, C.E. Cameron, J.Y.N. Lau, Z. Hong, J. Virol. 74 (2000) 9134–9143.